SUPPLEMENTARY MATERIAL

Thermal state of the upper mantle and the origin of the Cambrian-Ordovician ophiolite pulse: constraints from ultramafic dikes of the Hayachine-Miyamori Ophiolite

TAKAFUMI KIMURA[1], KAZUHITO OZAWA[1], TAKESHI KURITANI[2], TSUYOSHI IIZUKA[1], AND MITSUHIRO NAKAGAWA[2]

Affiliations:

Corresponding author: Takafumi Kimura

e-mail address: kimura.t@eps.s.u-tokyo.ac.jp

phone numbers: +81-3-5841-4021

SUPPLEMENTARY FIGURES

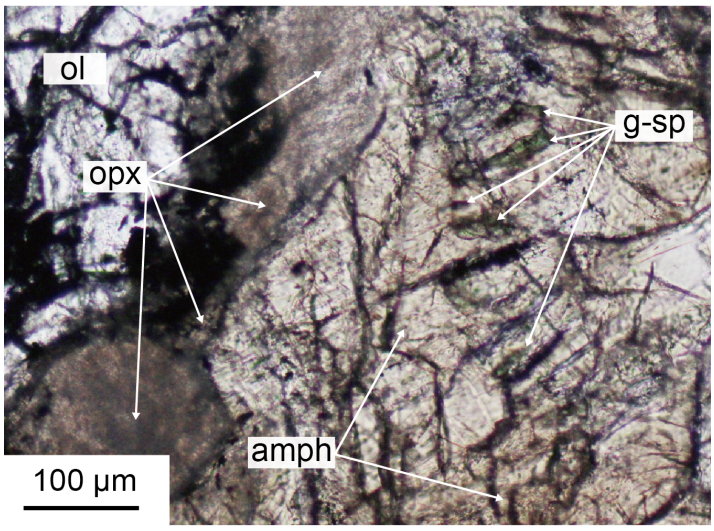

Fig. S1: Photomicrograph (open nicol) of a thin section made from DKSH2. Orthopyroxene (opx) is totally altered into darker fine-grained aggregate. Anhedral green spinel (g-sp) grains are vermicular in morphology and included in amphibole grains (amph).

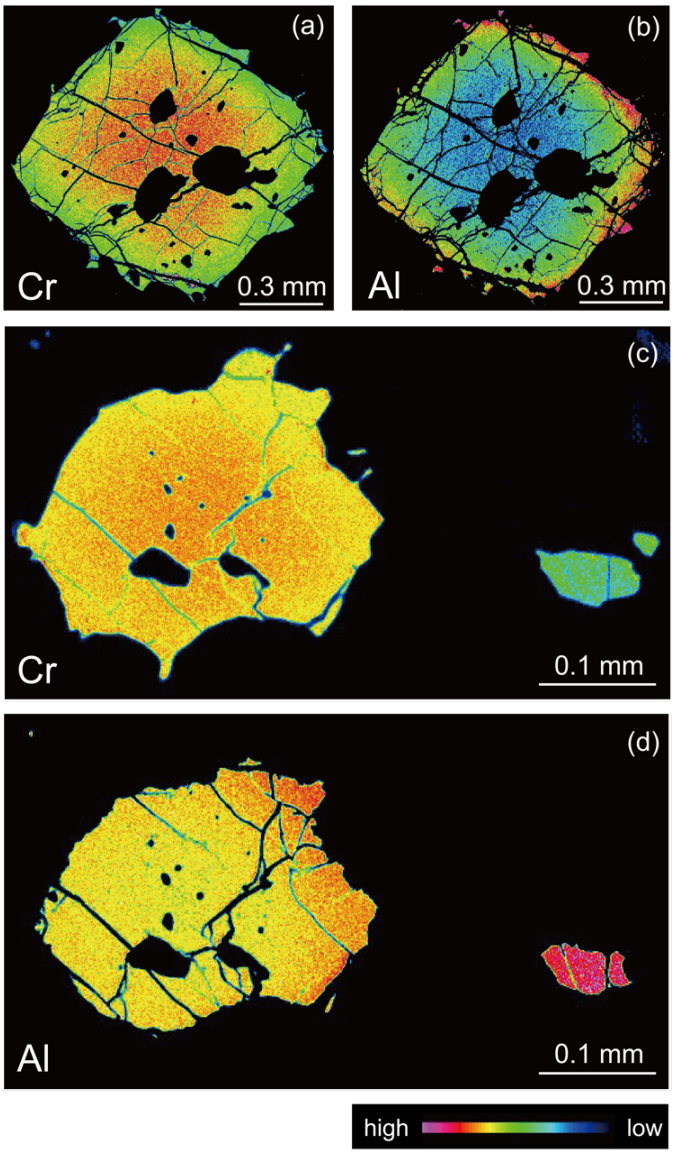

Fig. S2: X-ray intensity maps of a euhedral spinel grain for Cr (a) and Al (b) and subhedral to anhedral grains for Cr (c) and Al (d) in dike DKSH2. Black spots in spinel grains are clinopyroxene inclusions. The spinel grains in (c) and (d) occur near a plagioclase pseudomorph, which is 1 mm far right of the smaller grain. Note that the large euhedral spinel grain in (a) and (b) shows a concentric Al-Cr zoning with decreasing Cr# from the core to the rim (from 0.37 at the core to 0.07 at the rim). Note also that the large subhedral spinel grain in (c) and (d) shows asymmetric zoning in Al and Cr with notable enrichment of Al

towards the rim closer to the small very Al-rich and Cr-poor spinel grain on the right, which is greenish in color. A part of the small spinel grain is replaced by ferritechromite owing to low-temperature alteration, and is very low in Al with keeping Cr, which results in its disappearance in (d).

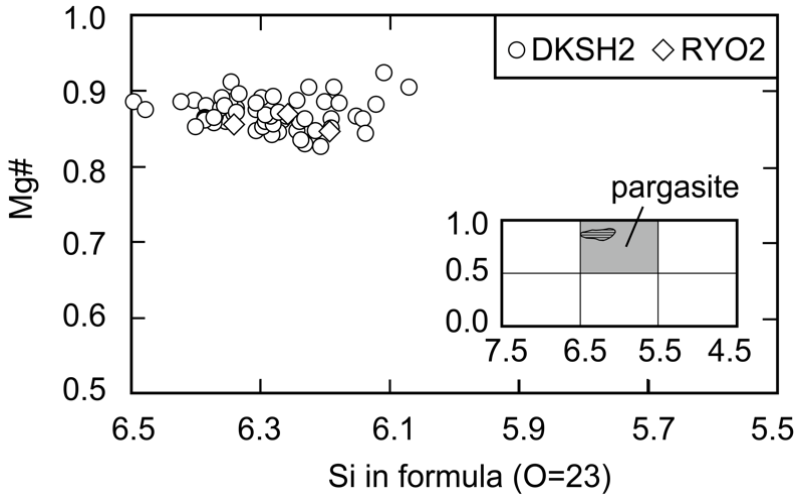

Fig. S3: Chemical compositions of amphibole forming the matrix in the examined dikes plotted in classification diagram after Leake et al. (1997). Circle and diamond are the same as those used in Fig. 4. They are all classified as pargasite with wide variations in Si (6.0 - 6.5) and Mg# (0.82 - 0.92).

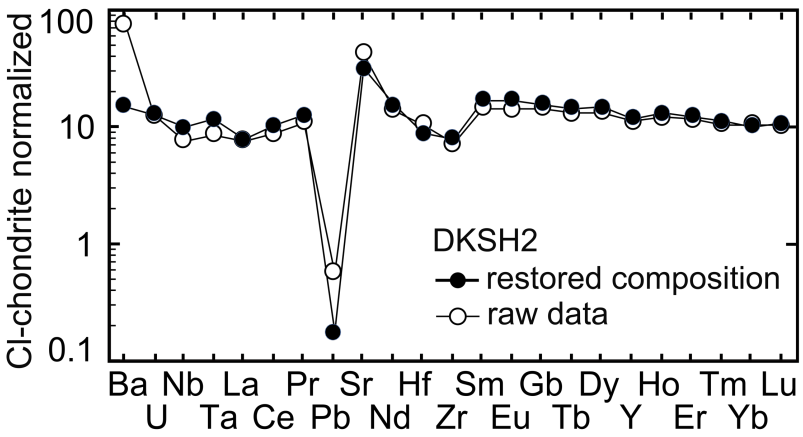

Fig. S4: Chondrite-normalized trace element patterns of the intruded melts for the dike (DKSH2) estimated from amphibole and clinopyroxene compositions and their modal abundances in the matrix (solid circles, Tables 5 and 6) and the bulk composition directory measured with ICP-MS (open circles; DKSH2 in Table 5).

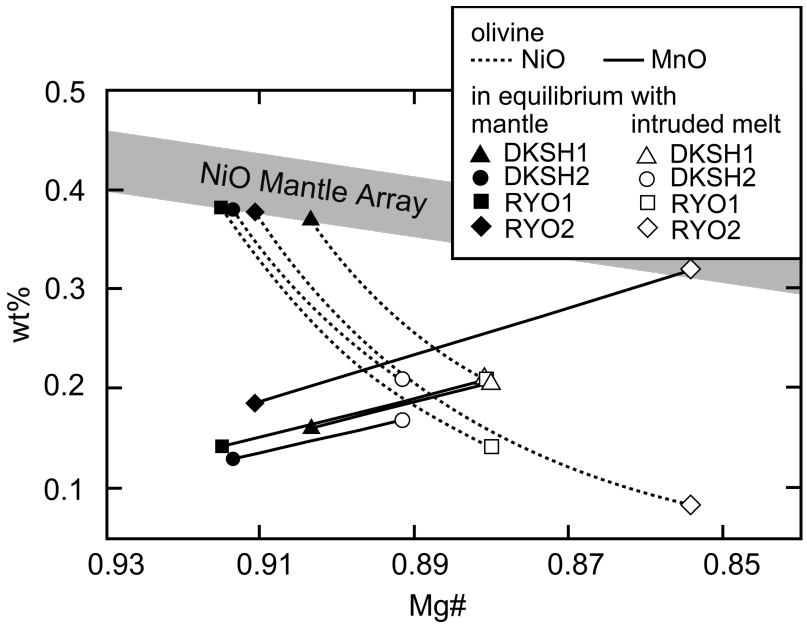

Fig. S5: Relationships of NiO and MnO wt% against Mg# of olivine to show our estimation procedure for constraining olivine compositions in equilibrium with residual peridotites after production of the primary melts for the examined 4 ultramafic dikes (DKSH1, open triangle; DKSH2, open circle; RYO1, open square; and RYO2, open diamond). Open symbols represent olivine compositions in equilibrium with the intruded melts (Table 5). Starting from these compositions, compositions of olivine in equilibrium with the residual peridotite (solid symbols) are estimated by adding olivine according to the maximum olivine fractionation model as shown by dashed lines for NiO and solid lines for MnO until reaching the lower edge of the olivine mantle array for Mg#-NiO after Takahashi and Uto (1987) (shaded region) by using partition coefficients after Beattie et al. (1991) and Kinzler et al. (1990).

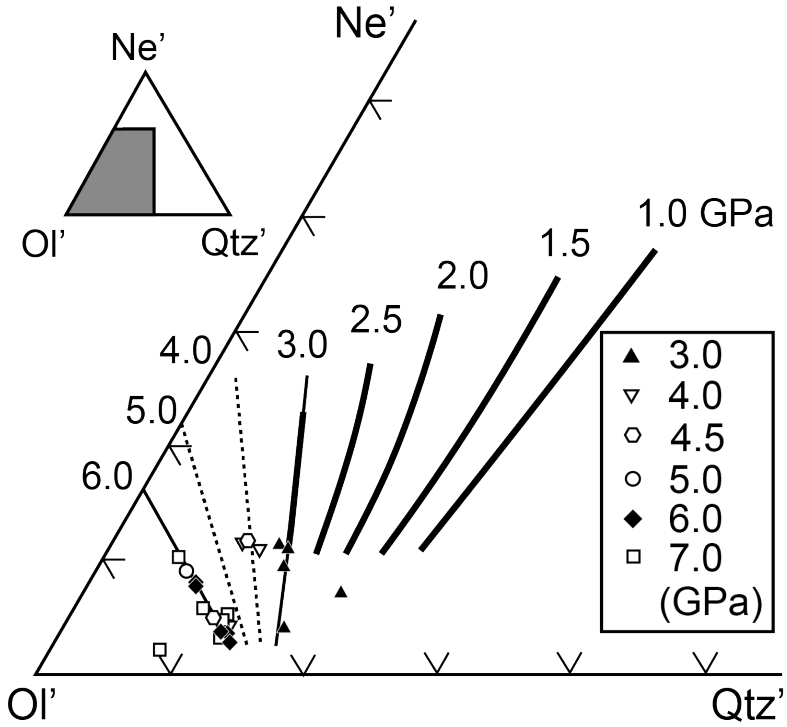

Fig. S6: Pressure isopleths in the ternary nepheline (Ne')-olivine (Ol')-quartz (Qtz') normative composition for primary melts experimentally reproduced under anhydrous conditions to be in equilibrium with mantle peridotites. In addition to the isopleths for pressure ≤ 3.0 GPa shown with thick solid lines after Sakuyama et al. (2009), those for pressure at 3.0 and 6.0 GPa shown with solid lines are obtained by fitting experimental results at these pressures after Walter (1998) and extending the trend to the lower degree of melting region. We chose the 3 GPa results because the experiments were conducted by using piston-cylinder experimental apparatus, though we ignored one outlier with the highest SiO_2 content, which is peculiar in that orthopyroxene was not present in the residue (Walter, 1998). The 3 GPa isopleth based on Walter (1998) lies on the extension of that of Sakuyama et al. (2009) for lower degree of melting. We chose the results of 6 GPa experiments conducted by using multi-anvil high-pressure apparatuses because the results give a consistent trend in the ternary plot systematically decreasing Ne' with temperature and melting degree. We did not use the results of 5 and 7 GPa experiments, which are mostly overlapping with those of 6GPa

experiments. They give very scattered results in the ternary plot and are contrasting to the consistent results of 6 GPa experiments. The isopleths for 4 and 5 GPa isopleths shown with dashed lines are obtained by a linear interpolation of 3 and 6 GPa isopleths, which is consistent with 4 GPa experimental results. The projection scheme is after Irvine and Barager (1971): Ne' = Nepheline + 0.6Albite; Qtz' = Quartz + 0.4 Albite + 0.25 Orthopyroxene; Ol' = Olivine + 0.75 Orthopyroxene.

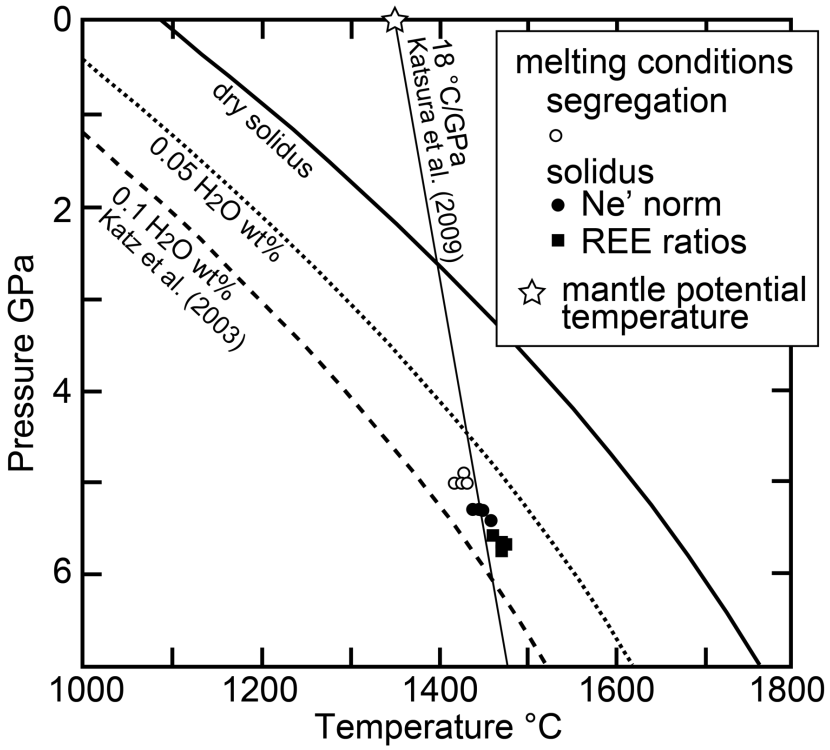

Fig. S7: Estimated melting conditions and mantle potential temperature (MPT) for the ultramafic dikes compared with the water-present solidi after Katz et al. (2003). The solidus conditions (solid circles and squares) are estimated from the segregation conditions (open circles: 1420 – 1430 °C, 4.9 – 5.0 GPa), the melting adiabats (Table S7), and the melting degrees estimated by two methods. We obtained the solidus conditions as 1440 -1460 °C, 5.3 - 5.4 GPa, and 0.04 - 0.18 H_2Owt% in the mantle source (solid circles) by using melting degree of 7.1 – 8.7 % based on the Ne' norm (Fig. 16) and as 1460 -1480 °C, 5.6 - 5.8 GPa, and 0.11 - 0.31 H_2Owt% in the mantle source (solid squares) by using melting degree of 13.7 – 20.0 % based on the relationships between (Nd/Sm)n and (Dy/Yb)n (Table 7 and Table S2). The solidus conditions are plotted along the water-present solidus for ~0.08 wt% H_2O according to Katz et al. (2003). The water content is more consistent with that calculated by using Ne' norm. We, therefore, accepted the former melting conditions more plausible, and the mean temperature and pressure (~1450 °C and ~5.3 GPa) give MPT of ~1350 °C by extrapolating to 1 bar along the solid mantle adiabat (18 °C/GPa; Katsura et al., 2009).

SUPPLEMENTARY TABLES

Table S1: Slopes defined by the difference in oxide contents of two samples from dike DKSH2 with a large contrast in degree of alteration in the diagram of oxides wt% plotted against loss on ignition (LOI) (Fig. 11: e.g., Al_2O_3, MgO, and Fe_2O_3). The slope values represent relative changes of major oxide wt% to an increase in the loss on ignition LOI.

	slopes ($\times 10^{-2}$)
SiO_2	- 7.03
TiO_2	- 2.86
Al_2O_3	85.75
Fe_2O_3	6.88
MnO	- 0.22
MgO	- 88.61
CaO	- 21.08
Na_2O	24.91
K_2O	2.82
P_2O_5	0.01
NiO	- 0.50
Cr_2O_3	- 0.08

Table S2: Partition coefficients of rare earth and other trace elements between melts and minerals used in the melting models (Figs. 14 and 18). The data are after Beattie (1994), (1993), Hart and Dunn (1993), Green (1994), McKenzie and O'Nions (1991), Kennedy et al. (1993), Matsui et al. (1977), Ozawa and Shimizu (1995), Hauri et al. (1994), Jenner et al. (1993), Johnson (1994), Frey (1969), Skulski et al. (1994), Kelemen et al. (1990), Dunn and Sen (1994), Kelemen and Dunn (1992), Nicholls and Harris (1990), Irving and Frey (1984), Fujimaki et al. (1984), Colson et al. (1988), and Nikogosyan and Sobolev (1997).

	olivine	spinel	orthopyroxene	clinopyroxene	garnet
Ba	0.000032	0.	0.0035	0.0006	0.0007
U	0.000018	0.	0.0017	0.00361	0.00918
Nb	0.0001	0.02	0.003	0.0077	0.015
Ta	0.00007	0.02	0.003	0.0102	0.02
Pb	0.00048	0.	0.0013	0.072	0.0005
Sr	0.0015	0.	0.007	0.1283	0.006
Hf	0.0038	0.02	0.01	0.256	0.24
Zr	0.007	0.02	0.021	0.123	0.5
La	0.000028	0.01	0.0025	0.054	0.0015
Ce	0.000038	0.01	0.005	0.086	0.008
Pr	0.0008	0.01	0.0048	0.15	0.054
Nd	0.00042	0.01	0.0068	0.19	0.087
Sm	0.0013	0.008	0.01	0.29	0.7
Eu	0.0016	0.007	0.013	0.31	0.9
Gd	0.0055	0.006	0.016	0.3	1.19
Tb	0.0041	0.009	0.019	0.31	1.5
Dy	0.01	0.01	0.022	0.33	2.2
Ho	0.007	0.009	0.026	0.31	3.3
Er	0.0087	0.01	0.03	0.29	3.6
Tm	0.009	0.01	0.12	0.26	3.5
Yb	0.017	0.008	0.05	0.28	3.9
Lu	0.02	0.02	0.06	0.28	3.8

Table S3: Optimized set of model parameters for one-dimensional steady-state decompressional fractional melting models without material influx and the assumed initial mineral modes and meltin modes for DKSH1.

Dike: DKSH1

Source: Primitive mantle

Strength of melt separation: Accumulated

Percentage of melting at the garnet stability field in F (wt%): 95.7

Stage	Melting mode				
	Olivine	Spinel	Orthopyroxene	Clinopyroxene	Garnet
garnet	0.08	0.00	-0.19	0.81	0.30
spinel	-0.34	0.13	0.46	0.75	0.00

Stage	Lithology	Parameters for open system melting model	
		α [1]	γ [1]
1	Gt lhz	0.000	0.000
2	Gt lhz	0.005	0.900
3	Gt lhz	0.020	0.900
4	Gt/Sp lhz	0.150	1.000

Source: MORB like mantle

Strength of melt separation: Accumulated

Percentage of melting at the garnet stability field in F (wt%): 88.7

Stage	Melting mode				
	Olivine	Spinel	Orthopyroxene	Clinopyroxene	Garnet
garnet	0.08	0.00	-0.19	0.81	0.30
spinel	-0.34	0.13	0.46	0.75	0.00

Stage	Lithology	Parameters for open system melting model	
		α	γ
1	Gt lhz	0.000	0.000
2	Gt lhz	0.005	0.010
3	Gt lhz	0.020	1.000
4	Gt/Sp lhz	0.150	1.000

Source: MORB like mantle

Strength of melt separation: Instantaneous

Percentage of melting at the garnet stability field in F (wt%): 99.9

Stage	Melting mode				
	Olivine	Spinel	Orthopyroxene	Clinopyroxene	Garnet
garnet	0.08	0.00	-0.19	0.81	0.30
spinel	-0.34	0.13	0.46	0.75	0.00

Stage	Lithology	Parameters for open system melting model	
		α	γ
1	Gt lhz	0.000	0.000
2	Gt lhz	0.005	0.100
3	Gt lhz	0.020	0.400
4	Gt/Sp lhz	0.150	1.000

Source: Depleted MORB like mantle

Strength of melt separation: Accumulated

Percentage of melting at the garnet stability field in F (wt%): 87.3

Stage	Melting mode				
	Olivine	Spinel	Orthopyroxene	Clinopyroxene	Garnet
garnet	0.08	0.00	-0.19	0.81	0.30
spinel	-0.34	0.13	0.46	0.75	0.00

Stage	Lithology	Parameters for open system melting model	
		α	γ
1	Gt lhz	0.000	0.000
2	Gt lhz	0.005	0.200
3	Gt lhz	0.020	0.900
4	Gt/Sp lhz	0.150	1.000

[1] α, and γ are the mass fraction of melt in the current system of the melting stage, and the separation rate, respectively. Gt lhz and Gt/Sp lhz are garnet lherzolite and spinel lherzolite.

Table S4: Optimized set of model parameters for one-dimensional steady-state decompressional fractional melting models without material influx and the assumed initial mineral modes and meltir modes for DKSH2.

Dike: DKSH2

Source: Primitive mantle

Strength of melt separation: Accumulated

Percentage of melting at the garnet stability field in F (wt%): 89.2

Stage	Melting mode				
	Olivine	Spinel	Orthopyroxene	Clinopyroxene	Garnet
garnet	0.08	0.00	-0.19	0.81	0.30
spinel	-0.34	0.13	0.46	0.75	0.00

Stage	Lithology	Parameters for open system melting model	
		α [1]	γ [1]
1	Gt lhz	0.000	0.000
2	Gt lhz	0.005	0.900
3	Gt lhz	0.020	0.900
4	Gt/Sp lhz	0.150	1.000

Source: MORB like mantle

Strength of melt separation: Accumulated

Percentage of melting at the garnet stability field in F (wt%): 76.6

Stage	Melting mode				
	Olivine	Spinel	Orthopyroxene	Clinopyroxene	Garnet
garnet	0.08	0.00	-0.19	0.81	0.30
spinel	-0.34	0.13	0.46	0.75	0.00

Stage	Lithology	Parameters for open system melting model	
		α	γ
1	Gt lhz	0.000	0.000
2	Gt lhz	0.005	0.900
3	Gt lhz	0.020	0.900
4	Gt/Sp lhz	0.150	1.000

Source: MORB like mantle

Strength of melt separation: Instantaneous

Percentage of melting at the garnet stability field in F (wt%): 99.9

Stage	Melting mode				
	Olivine	Spinel	Orthopyroxene	Clinopyroxene	Garnet
garnet	0.08	0.00	-0.19	0.81	0.30
spinel	-0.34	0.13	0.46	0.75	0.00

Stage	Lithology	Parameters for open system melting model	
		α	γ
1	Gt lhz	0.000	0.000
2	Gt lhz	0.005	0.200
3	Gt lhz	0.020	0.010
4	Gt/Sp lhz	0.150	1.000

Source: Depleted MORB like mantle

Strength of melt separation: Accumulated

Percentage of melting at the garnet stability field in F (wt%): 75.5

Stage	Melting mode				
	Olivine	Spinel	Orthopyroxene	Clinopyroxene	Garnet
garnet	0.08	0.00	-0.19	0.81	0.30
spinel	-0.34	0.13	0.46	0.75	0.00

Stage	Lithology	Parameters for open system melting model	
		α	γ
1	Gt lhz	0.000	0.000
2	Gt lhz	0.005	0.900
3	Gt lhz	0.020	1.000
4	Gt/Sp lhz	0.150	1.000

[1] α, and γ are the mass fraction of melt in the current system of the melting stage, and the separation rate, respectively. Gt lhz and Gt/Sp lhz are garnet lherzolite and spinel lherzolite.

Table S5: Optimized set of model parameters for one-dimensional steady-state decompressional fractional melting models without material influx and the assumed initial mineral modes and melting modes for RYO1.

Dike: RYO1

Source: Primitive mantle

Strength of melt separation: Accumulated

Percentage of melting at the garnet stability field in F (wt%): 97.2

Stage	Melting mode				
	Olivine	Spinel	Orthopyroxene	Clinopyroxene	Garnet
garnet	0.08	0.00	-0.19	0.81	0.30
spinel	-0.34	0.13	0.46	0.75	0.00

Stage	Lithology	Parameters for open system melting model	
		α [1]	γ [1]
1	Gt lhz	0.000	0.000
2	Gt lhz	0.005	0.900
3	Gt lhz	0.020	0.900
4	Gt/Sp lhz	0.150	1.000

Source: MORB like mantle

Strength of melt separation: Accumulated

Percentage of melting at the garnet stability field in F (wt%): 90.1

Stage	Melting mode				
	Olivine	Spinel	Orthopyroxene	Clinopyroxene	Garnet
garnet	0.08	0.00	-0.19	0.81	0.30
spinel	-0.34	0.13	0.46	0.75	0.00

Stage	Lithology	Parameters for open system melting model	
		α	γ
1	Gt lhz	0.000	0.000
2	Gt lhz	0.005	0.900
3	Gt lhz	0.020	0.900
4	Gt/Sp lhz	0.150	1.000

Source: MORB like mantle

Strength of melt separation: Instantaneous

Percentage of melting at the garnet stability field in F (wt%): 99.9

Stage	Melting mode				
	Olivine	Spinel	Orthopyroxene	Clinopyroxene	Garnet
garnet	0.08	0.00	-0.19	0.81	0.30
spinel	-0.34	0.13	0.46	0.75	0.00

Stage	Lithology	Parameters for open system melting model	
		α	γ
1	Gt lhz	0.000	0.000
2	Gt lhz	0.005	0.600
3	Gt lhz	0.020	0.400
4	Gt/Sp lhz	0.150	1.000

Source: Depleted MORB like mantle

Strength of melt separation: Accumulated

Percentage of melting at the garnet stability field in F (wt%): 93.0

Stage	Melting mode				
	Olivine	Spinel	Orthopyroxene	Clinopyroxene	Garnet
garnet	0.08	0.00	-0.19	0.81	0.30
spinel	-0.34	0.13	0.46	0.75	0.00

Stage	Lithology	Parameters for open system melting model	
		α	γ
1	Gt lhz	0.000	0.000
2	Gt lhz	0.005	0.200
3	Gt lhz	0.020	1.000
4	Gt/Sp lhz	0.150	1.000

[1] α, and γ are the mass fraction of melt in the current system of the melting stage, and the separation rate, respectively. Gt lhz and Gt/Sp lhz are garnet lherzolite and spinel lherzolite.

Table S6: Optimized set of model parameters for one-dimensional steady-state decompressional fractional melting models without material influx and the assumed initial mineral modes and meltir modes for RYO2.

Dike: RYO2

Source: Primitive mantle

Strength of melt separation: Accumulated

Percentage of melting at the garnet stability field in F (wt%): 98.0

Stage	Melting mode				
	Olivine	Spinel	Orthopyroxene	Clinopyroxene	Garnet
garnet	0.08	0.00	-0.19	0.81	0.30
spinel	-0.34	0.13	0.46	0.75	0.00

Stage	Lithology	Parameters for open system melting model	
		α [1]	γ [1]
1	Gt lhz	0.000	0.000
2	Gt lhz	0.005	0.900
3	Gt lhz	0.020	0.900
4	Gt/Sp lhz	0.150	1.000

Source: MORB like mantle

Strength of melt separation: Accumulated

Percentage of melting at the garnet stability field in F (wt%): 93.9

Stage	Melting mode				
	Olivine	Spinel	Orthopyroxene	Clinopyroxene	Garnet
garnet	0.08	0.00	-0.19	0.81	0.30
spinel	-0.34	0.13	0.46	0.75	0.00

Stage	Lithology	Parameters for open system melting model	
		α	γ
1	Gt lhz	0.000	0.000
2	Gt lhz	0.005	0.100
3	Gt lhz	0.020	1.000
4	Gt/Sp lhz	0.150	1.000

Source: MORB like mantle

Strength of melt separation: Instantaneous

Percentage of melting at the garnet stability field in F (wt%): 99.9

Stage	Melting mode				
	Olivine	Spinel	Orthopyroxene	Clinopyroxene	Garnet
garnet	0.08	0.00	-0.19	0.81	0.30
spinel	-0.34	0.13	0.46	0.75	0.00

Stage	Lithology	Parameters for open system melting model	
		α	γ
1	Gt lhz	0.000	0.000
2	Gt lhz	0.005	0.400
3	Gt lhz	0.020	0.700
4	Gt/Sp lhz	0.150	1.000

Source: Depleted MORB like mantle

Strength of melt separation: Accumulated

Percentage of melting at the garnet stability field in F (wt%): 93.9

Stage	Melting mode				
	Olivine	Spinel	Orthopyroxene	Clinopyroxene	Garnet
garnet	0.08	0.00	-0.19	0.81	0.30
spinel	-0.34	0.13	0.46	0.75	0.00

Stage	Lithology	Parameters for open system melting model	
		α	γ
1	Gt lhz	0.000	0.000
2	Gt lhz	0.005	0.100
3	Gt lhz	0.020	1.000
4	Gt/Sp lhz	0.150	1.000

[1] α, and γ are the mass fraction of melt in the current system of the melting stage, and the separation rate, respectively. Gt lhz and Gt/Sp lhz are garnet lherzolite and spinel lherzolite.

Table S7: Calculated adiabatic gradients, $(\partial F/\partial T)_S$ and parameters to estimate solidus conditions: temperature change for melting dgree (F), ΔT; thermal expansion, α for solid and melt; partial volume, V for solid and melt; heat capacity, Cp for solid and melt; and enthalpy change of melting, ΔH; increase in melting degree with temperature increase at constant pressure, $(\partial F/\partial T)_P$; increase in temperature with pressure increase at constant melting degree, $(\partial T/\partial P)_F$.

Dike:	DKSH1	DKSH2	RYO1	RYO2	data source
$(\partial F/\partial T)_S$ [K/GPa]	57.8	58.5	58.1	58.3	
ΔT for F [K]	20.4	24.9	20.5	21.5	Takahashi et al. (1993)
α^L (10^5) [1/K]	10.9	11.2	10.7	10.9	Fei (1995)
V^L [kJ/GPa]	219	217	219	220	Lange and Carmichael (1987)
Cp^L [J/Mol/K]	95.2	94.7	94.7	95.9	Stebbins et al. (1984)
α^S (10^5) [1/K]			4.0		Fei (1995)
V^S [kJ/GPa]			45.9		Berman (1998), Berman and Brown (1985)
Cp^S [J/Mol/K]			193.2		Berman (1998), Berman and Brown (1985)
ΔH [kJ/Mol]			97.3		Kojitani and Akaogi (1997)
$(\partial F/\partial T)_P$ (10^3) [1/K]			3.8		Takahashi et al. (1993)
$(\partial T/\partial P)_F$ [K/GPa]			64.2		McKenzie and Bickle (1988)